

# Structural investigation of Ni–Nb–Ti–Zr–Co–Cu glassy samples prepared by different welding techniques

D.V. Louzguine-Luzgin<sup>a,\*</sup>, G.Q. Xie<sup>a</sup>, T. Tsumura<sup>b</sup>, H. Fukuda<sup>b</sup>,  
K. Nakata<sup>b</sup>, H.M. Kimura<sup>a</sup>, A. Inoue<sup>a</sup>

<sup>a</sup> Institute for Materials Research, Tohoku University, Katahira 2-1-1, Aoba-Ku, Sendai 980-8577, Japan

<sup>b</sup> Joining & Welding Research Institute, Osaka University, Mihogaoka, Ibaraki, Osaka 567-0047, Japan

Received 22 May 2007; received in revised form 13 August 2007; accepted 3 September 2007

## Abstract

Although, bulk metallic glasses exhibit remarkable mechanical, physical and chemical properties, their critical size (the largest size of fully glassy sample produced by casting) is limited. The utilization of a welding technique enables producing larger glassy samples. Ni<sub>53</sub>Nb<sub>20</sub>Ti<sub>10</sub>Zr<sub>8</sub>Co<sub>6</sub>Cu<sub>3</sub> glassy alloy ribbon samples prepared by melt spinning of the pre-alloyed arc-melted ingots were welded by the electron-beam and fiber laser-beam welding techniques. The detailed structural investigations of the welded bead and thermally affected zone were performed by micro-area X-ray diffractometry, scanning and transmission electron microscopy. At certain optimized welding conditions the amorphous structure can be retained after melting. The obtained data are promising for future applications of the laser and electron-beam welding techniques to glassy alloys.

© 2007 Elsevier B.V. All rights reserved.

**Keywords:** Amorphous materials; Electron microscopy; Metastable phases

## 1. Introduction

Metallic glassy alloys (or metallic glasses) were initially produced using a rapid solidification technique for casting of metallic liquids at a very high solidification rate of 10<sup>6</sup> K/s [1]. However, a large number of bulk glassy alloys (also called bulk metallic glasses) defined as three-dimensional massive glassy (amorphous) articles with a size of not less than 1 mm in any dimension have been produced during the last years [2–4]. These alloys are promising materials for structural applications as they exhibit high mechanical strength, high hardness, good fracture toughness, good corrosion resistance [2], etc.

Recently, Ni-based glassy alloys were formed in Ni–Zr–Ti–(Si,Sn) [5], Ni–Nb–Ti–Zr [6], Ni–Nb–Ti [7], Ni–Nb–Sn [8] and some other systems. These alloys demonstrate a high strength of 2.5–3 GPa. The devitrification behavior of Ni–Nb–Ti [9], Ni–Nb–Ti–Zr and Ni–Nb–Ti–Zr–Pt [10] glassy alloys has been studied recently.

A limited size of bulk metallic glassy samples requires bonding technology to obtain industrial-size samples. Weld-

ing of Zr-based and Pd-based bulk glassy alloys has been achieved by Joule heating [11,12]. Electron-beam welding of Zr<sub>50</sub>Cu<sub>30</sub>Ni<sub>10</sub>Al<sub>10</sub> bulk glassy alloy having no distinct crystallized regions has also been accomplished [13]. Welding of metallic glassy samples with metals has been performed using explosion, pulse-current and electron-beam methods [14]. In the present work, we study the welding behavior of the Ni<sub>53</sub>Nb<sub>20</sub>Ti<sub>10</sub>Zr<sub>8</sub>Co<sub>6</sub>Cu<sub>3</sub> glassy alloy [15].

## 2. Experimental procedure

An ingot of the Ni<sub>53</sub>Nb<sub>20</sub>Ti<sub>10</sub>Zr<sub>8</sub>Co<sub>6</sub>Cu<sub>3</sub> alloy was prepared by arc-melting using pure elements in an argon atmosphere. From this ingot a metallic glassy ribbon of 40 mm in width and 0.025 mm in thickness was produced by rapid solidification of the melt on a single copper roller at a roller tangential velocity of 40 m/s. The structure of the samples was examined by X-ray diffractometry (XRD) with monochromatic Cu K $\alpha$  radiation. The structure of the welded sample was studied using a micro-area XRD with a collimator size of 30  $\mu$ m. The phase transformations were studied by differential scanning calorimetry (DSC) at a heating rate of 0.67 K/s and differential isothermal calorimetry (DIC).

\* Corresponding author. Tel.: +81 22 215 2220; fax: +81 22 215 2111.

E-mail address: dml@imr.tohoku.ac.jp (D.V. Louzguine-Luzgin).

Laser-beam welding was carried out by fiber laser welding in the atmosphere at laser power of 120 W, wave length of the laser of 1070 nm, spot diameter of 0.3 mm, slit width of the cover plate of 0.6 mm and at the welding speed of 6 m/min.

The electron beam welding was carried out at the accelerating voltage of 60 kV, beam current range of 3.9 mA, welding speed of 4 m/min under an evacuated atmosphere of about 0.1 Pa. In order to prevent crystallization at the heat affected zone copper plates were used as the cover and backing plates.

Transmission electron microscopy (TEM) investigation was carried out using a JEM 2010 (JEOL) microscope operating at 200 kV equipped with an energy dispersive X-ray (EDX) spectrometer of 0.1 keV resolution. The samples for TEM were prepared by the ion-polishing technique. Scanning electron microscopy (SEM) investigations were carried out at 15 kV.

### 3. Results and discussion

Fig. 1(a) shows a DSC trace of the  $\text{Ni}_{53}\text{Nb}_{20}\text{Ti}_{10}\text{Zr}_8\text{Co}_6\text{Cu}_3$  glassy alloy obtained at 0.67 K/s while Fig. 1(b) represents a part of the corresponding isothermal transformation curve created using DIC traces obtained at 873, 865 and 855 K. This figure represents the thermal stability of the glassy alloy upon continuous heating and in the isothermal mode. On heating above the crystallization temperature or after holding for a certain time at the elevated temperature the hR14  $\text{Ni}_4\text{Ti}_3$ -type crystalline phase precipitates due to thermodynamic instability of the glassy phase.

The  $\text{Ni}_{53}\text{Nb}_{20}\text{Ti}_{10}\text{Zr}_8\text{Co}_6\text{Cu}_3$  glassy alloy has a large super-cooled liquid region (Fig. 1(a)) which indicates its relatively

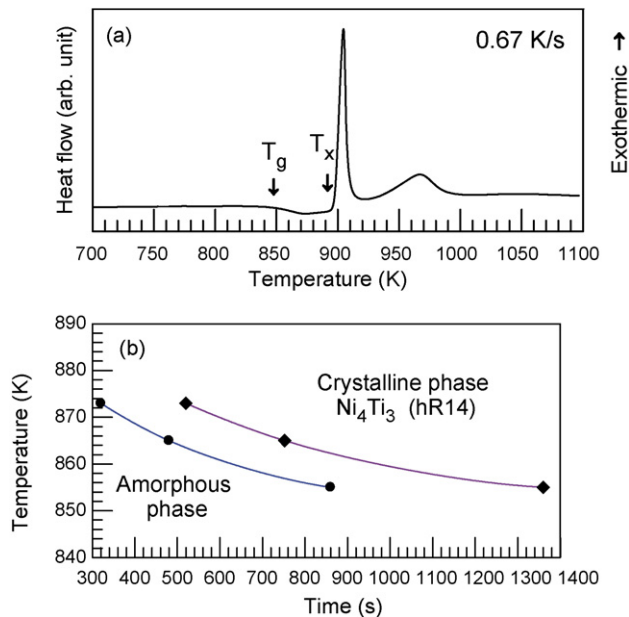


Fig. 1. (a) DSC trace of the  $\text{Ni}_{53}\text{Nb}_{20}\text{Ti}_{10}\text{Zr}_8\text{Co}_6\text{Cu}_3$  alloy obtained at 0.67 K/s. (b) The part of the corresponding isothermal transformation curve obtained using isothermal calorimetry.

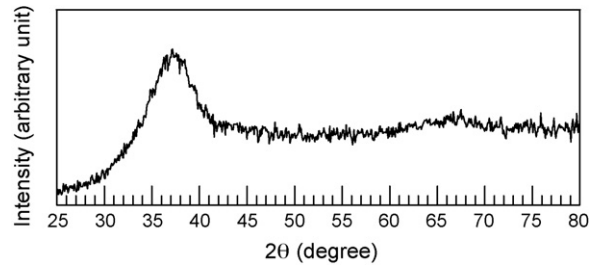


Fig. 2. Micro-area XRD spectrum taken from the weld bead of the sample welded by fiber laser welding.

high thermal stability compared to other glassy alloys and capability for welding. The micro-area XRD pattern taken from the weld bead of the laser-welded sample is shown in Fig. 2. Similar diffraction patterns were obtained from various places within the heat-affected zone taken 0.5, 1, 2 and 3 mm apart from the weld bead.

High-resolution TEM image taken from the weld bead area of the sample welded by the fiber laser welding at 120 W is presented in Fig. 3. It demonstrates typically amorphous irregular structure which is also confirmed by using the nanobeam diffraction pattern (NBD), though some weak spot-like features within the amorphous halo indicate a certain degree of medium-range order (MRO) which typically exists on 0.5–1 nm length scale.

At the same time some spherical micron scale particles were found embedded (Fig. 4) in the glassy matrix in some areas. The selected-area electron-diffraction (SAED) pattern was successfully indexed according to mp12  $\text{ZrO}_2$  lattice [16]. These particles were also observed in the SEM micrograph of the polished cross-section. SEM technique allowed us to calculate the volume fraction of  $\text{ZrO}_2$  particles to be about 1 vol.%. The EDX spectroscopy revealed the composition of such particles to be

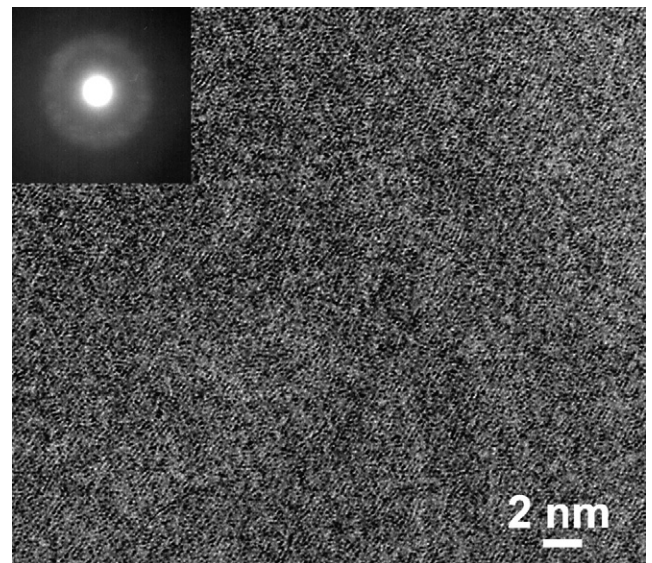


Fig. 3. High-resolution TEM image taken from the weld bead area of the sample welded by the fiber laser welding. The insert is NBD pattern.

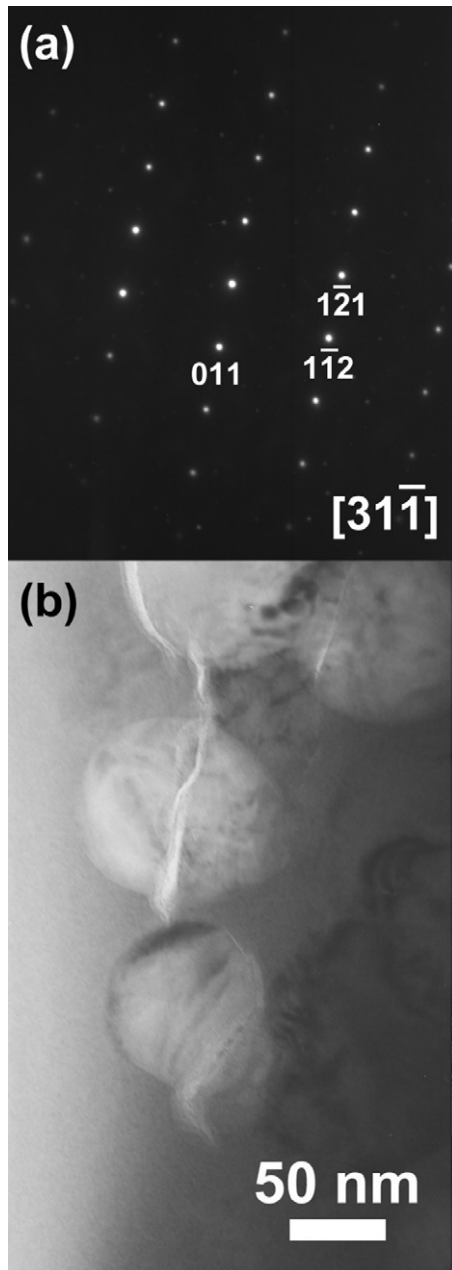


Fig. 4. (a) SAED pattern taken from a particle in the bright-field TEM image (b) of the sample welded by the fiber laser welding.

close to the nominal composition. Nb is also dissolved in the  $\text{ZrO}_2$  compound partially substituting Zr.

According to XRD results no crystals were found in the samples obtained by the electron beam welding carried out at the accelerating voltage of 60 kV and the welding current of 3.9 mA. At the same time not only MRO zones but also the nanoparticles up to 3–4 nm in size can be observed by the high-resolution TEM taken from the weld bead area (Fig. 5). These particles belong to hR14  $\text{Ni}_4\text{Ti}_3$ -phase which was also formed primarily in the  $\text{Ni}_{53}\text{Nb}_{20}\text{Ti}_{10}\text{Zr}_8\text{Co}_6\text{Cu}_3$  glassy alloy on heating above the crystallization temperature. The volume fraction of the nanoparticles is estimated to be less than 10 vol.%. TEM observations do not

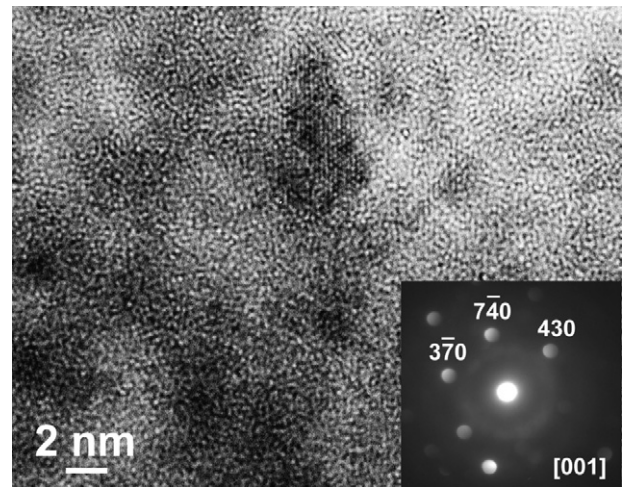


Fig. 5. High-resolution TEM image taken from the weld bead area of the sample welded by electron beam welding carried out at the accelerating voltage of 60 kV and the welding current of 3.9 mA. The insert represents the NBD pattern taken from the nanoparticle.

allow precise determination of the volume fraction while these particles are too small for SEM observation.

Almost fully amorphous samples were obtained with a small volume fraction of the hR14  $\text{Ni}_4\text{Ti}_3$  solid solution crystalline phase upon the electron-beam welding, though some surface oxidation was also observed.

The results of this work indicate successful welding of the  $\text{Ni}_{53}\text{Nb}_{20}\text{Ti}_{10}\text{Zr}_8\text{Co}_6\text{Cu}_3$  glassy alloy by the laser and electron-beam welding technique. The structure remained amorphous in the case of the laser-beam welding while a minor nanocrystallization is observed in the case of the electron-beam welding. In general, the energy density for the electron-beam is nearly equal to that for the fiber laser-beam. However, in this work, we applied the defocused electron-beam on the specimen surface because we need the less power than minimum for using the equipment. Considering the difference in the structure of the welded bead in the laser-beam and the electron-beam welded samples one can say that energy density of electron-beam is smaller than that of laser-beam. In other words on the fiber laser welding, the amount of energy is suitable for welding of this sample without crystallization as well as the cooling rate is high enough. On the other hand, in the electron-beam welding, the amount of energy is larger and the cooling rate is not enough to suppress the crystallization.

#### 4. Conclusion

Good bonding between two  $\text{Ni}_{53}\text{Nb}_{20}\text{Ti}_{10}\text{Zr}_8\text{Co}_6\text{Cu}_3$  glassy samples was obtained for the electron-beam samples welded at the beam current of 3.9 mA and voltage of 60 kV at the speed of 4 m/min and by 120 W fiber laser-beam, wavelength  $\lambda = 1.07 \mu\text{m}$  welding at the speed of 6 m/min. Almost fully amorphous samples with a small volume fraction of the hR14  $\text{Ni}_4\text{Ti}_3$  solid solution nanocrystalline phase were obtained upon the electron-beam welding, though some surface oxidation was

observed due to insufficient vacuum. In the case of the laser-beam welding no crystallization of the welded sample was found, though nearly 1 vol.% of ZrO<sub>2</sub> particles are found to be embedded in the glassy matrix. The results indicate that a good protection against oxidation is required for the studied alloy.

### Acknowledgement

This work was supported in part by the Research and Development Project on Advanced Metallic Glasses, Inorganic Materials and Joining Technology from Ministry of Education, Culture, Sports, Science and Technology, Japan.

### References

- [1] W. Clement, R.H. Willens, P. Duwez, *Nature* 187 (1967) 869–870.
- [2] A. Inoue, *Mater. Trans. JIM* 36 (1995) 866–875.
- [3] A. Inoue, *Acta Mater.* 48 (2000) 279–306.
- [4] W.L. Johnson, *MRS Bull* 24 (1999) 42–56.
- [5] S. Yi, T.G. Park, D.H. Kim, *J. Mater. Res.* 15 (2000) 2425–2429.
- [6] A. Inoue, W. Zhang, T. Zhang, *Mater. Trans.* 43 (2002) 1952–1956.
- [7] W. Zhang, A. Inoue, *Mater. Trans.* 43 (2002) 2342–2345.
- [8] H. Choi-Yim, D. Xu, W.L. Johnson, *Appl. Phys. Lett.* 82 (2003) 1030–1032.
- [9] T. Shimada, D.V. Louzguine, J. Saida, A. Inoue, *Mater. Trans.* 46 (2005) 675–680.
- [10] D.V. Louzguine-Luzgin, T. Shimada, A. Inoue, *Intermetallics* 13 (2005) 1166–1171.
- [11] M. de Oliveria, W.J. Botta F., A.R. Yavari, *Mater. Trans. JIM* 41 (2000) 1501.
- [12] A.R. Yavari, M.F. de Oliveira, C.S. Kiminami, A. Inoue, W.J. Botta, *Mater. Sci. Eng. A* 375–377 (2004) 227.
- [13] Y. Yokoyama, N. Abe, K. Fukaura, A. Inoue, *Mater. Trans. JIM* 43 (2002) 2509.
- [14] Y. Kawamura, *Mater. Sci. Eng. A* 375–377 (2004) 112.
- [15] T. Zhang, A. Inoue, *Mater. Trans. JIM* 43 (2002) 708–711.
- [16] B. Bondars, G. Heidemane, J. Grabis, K. Laschke, H. Boysen, J. Schneider, F. Frey, *J. Mater. Sci.* 30 (1995) 1621–1625.